Archival Report

Biological Psychiatry

Astrocytes Render Memory Flexible by Releasing D-Serine and Regulating NMDA Receptor Tone in the Hippocampus

Wuhyun Koh, Mijeong Park, Ye Eun Chun, Jaekwang Lee, Hyun Soo Shim, Mingu Gordon Park, Sunpil Kim, Moonsun Sa, Jinhyeong Joo, Hyunji Kang, Soo-Jin Oh, Junsung Woo, Heejung Chun, Seung Eun Lee, Jinpyo Hong, Jiesi Feng, Yulong Li, Hoon Ryu, Jeiwon Cho, and C. Justin Lee

ABSTRACT

BACKGROUND: NMDA receptor (NMDAR) hypofunction has been implicated in several psychiatric disorders with impairment of cognitive flexibility. However, the molecular mechanism of how NMDAR hypofunction with decreased NMDAR tone causes the impairment of cognitive flexibility has been minimally understood. Furthermore, it has been unclear whether hippocampal astrocytes regulate NMDAR tone and cognitive flexibility.

METHODS: We employed cell type–specific genetic manipulations, ex vivo electrophysiological recordings, sniffer patch recordings, cutting-edge biosensor for norepinephrine, and behavioral assays to investigate whether astrocytes can regulate NMDAR tone by releasing D-serine and glutamate. Subsequently, we further investigated the role of NMDAR tone in heterosynaptic long-term depression, metaplasticity, and cognitive flexibility.

RESULTS: We found that hippocampal astrocytes regulate NMDAR tone via BEST1-mediated corelease of D-serine and glutamate. *Best1* knockout mice exhibited reduced NMDAR tone and impairments of homosynaptic and α_1 adrenergic receptor–dependent heterosynaptic long-term depression, which leads to defects in metaplasticity and cognitive flexibility. These impairments in *Best1* knockout mice can be rescued by hippocampal astrocyte-specific BEST1 expression or enhanced NMDAR tone through D-serine supplement. D-serine injection in *Best1* knockout mice during initial learning rescues subsequent reversal learning.

CONCLUSIONS: These findings indicate that NMDAR tone during initial learning is important for subsequent learning, and hippocampal NMDAR tone regulated by astrocytic BEST1 is critical for heterosynaptic long-term depression, metaplasticity, and cognitive flexibility.

https://doi.org/10.1016/j.biopsych.2021.10.012

The flexibility of memory is as important as the formation of memory, because an environment and circumstances are not static but dynamically changing. When necessary, acquired memories should be flexibly adjusted to adapt to the changing environment. This ability is generally termed cognitive flexibility (1). Cognitive flexibility has been reported to decline in several diseases, for instance, autism spectrum disorder (2), schizophrenia (3), and early stages of Alzheimer's disease (AD) (4,5), in which a hypofunction of the NMDA receptor (NMDAR) is implicated (6–8). However, little is known about how NMDAR hypofunction affects cognitive flexibility.

In the hippocampus, NMDAR-dependent long-term depression (LTD) is proposed to be associated with spatial reversal learning (9–12), a hippocampus-dependent form of cognitive flexibility (13). Although this hypothesis is conceivable because hippocampal LTD is NMDAR dependent (14), reports of decreased cognitive flexibility with enhanced LTD (15) or increased cognitive flexibility with impaired LTD (16) suggest alternative mechanisms. However, studies of other mechanisms between NMDAR-dependent plasticity and cognitive flexibility have been poorly investigated.

D-serine, one of the coagonists that could constitute NMDAR tone, has been investigated in hippocampal LTD and cognitive flexibility. For example, it has been shown that endogenous D-serine plays an important role in the induction of hippocampal LTD (17), and that a D-serine increase by additional D-serine application or a loss-of-function mutation of D-amino acid oxidase, a key catabolic enzyme for D-serine, enhanced cognitive flexibility (12,18) or hippocampal LTD (12). While these results imply that D-serine–mediated NMDAR tone can facilitate cognitive flexibility, the precise molecular and cellular mechanism of how endogenous D-serine is regulated and facilitates cognitive flexibility is not fully understood. It is still unclear and controversial whether the cellular source of D-serine is astrocyte (19) or neuron (20).

Recently, optogenetic stimulation of astrocytes with channelrhodopsin-2 has been shown to induce an increase in hippocampal NMDAR tone (21) and NMDAR-dependent LTD

ISSN: 0006-3223

(22). This increase in NMDAR tone was reduced by the treatment of NPPB (21), which blocks anion channels, including the Ca^{2+}-activated, glutamate-permeable anion channel BEST1 (23), raising a possibility that BEST1-mediated glutamate release from astrocytes (24,25) might contribute to hippocampal NMDAR tone and LTD. In addition, norepinephrine (NE), which can stimulate astrocytic Ca^{2+} through the α_1 adrenoreceptor (α1-AR) (26), has been shown to induce NMDAR- and α1-AR–dependent LTD (NE-LTD) (27), recalling NMDA application (28). Chemogenetic activation of the locus coeruleus (LC) can restore cognitive flexibility in a model of early stages of AD (29), suggesting an important role of NE in cognitive flexibility. However, it has not been known whether NE induces NMDAR tone increase and NE-LTD through astrocytic Ca^{2+} activation and how astrocytic activation affects cognitive flexibility.

In addition, astrocytic activation can lead to not only homosynaptic LTD (22,30) but also heterosynaptic LTD (31), which was first documented to occur at unstimulated synapses accompanying homosynaptic long-term potentiation (LTP). Heterosynaptic LTD has great potential as the aforementioned alternative mechanism for cognitive flexibility, because it has been suggested to enable metaplasticity (32), a plasticity of synaptic plasticity (33,34). However, the molecular mechanism by which heterosynaptic LTD is regulated by astrocytes and how it contributes to cognitive flexibility has been poorly investigated.

In this study, we have investigated how astrocytes regulate heterosynaptic LTD and metaplasticity and thereby contribute to cognitive flexibility.

METHODS AND MATERIALS

See the Supplement for more details. All animal experiments except behavioral experiments were performed in 8- to 16-week-old male and female mice. For behavioral experiments, only male mice were used. Mice were given ad libitum access to food and water under a 12:12-hour light-dark cycle. All animal care and handling were performed according to the directives of the Institutional Animal Care and Use Committee of the Korea Institute of Science and Technology and Institute for Basic Science.

For electrophysiological recordings in acute brain slices, 350-μm-thick transverse or coronal slices were prepared. To measure tonic NMDAR current ($I_{tonicNMDAR}$), whole-cell voltage-clamp recording was performed holding at +40 mV. Baseline current was stabilized under treatment of CNQX (20 μM), bicuculline (10 μM), CGP55845 (10 μM), and strychnine (10 μM), and subsequently, $I_{tonicNMDAR}$ was measured by the baseline shift after 50 μM APV. Astrocytic Ca^{2+} chelation was performed as previously described (35).

For field excitatory postsynaptic potential (fEPSP) recordings in hippocampal slices, a 400- μm-thick transverse of hippocampal slices was prepared. The stimulation intensity was adjusted to obtain fEPSP slopes of 40% to 50% of the maximum. Basal fEPSP response was monitored at 0.067 Hz. For the simultaneous homosynaptic and heterosynaptic recordings, borosilicate theta glass was prepared to deliver focal stimulation on two independent pathways. Stimulation intensity was adjusted to acquire two independent pathways during a paired-pulse ratio test with 50-ms intervals, and the amplitude of each fEPSP was 0.1 to 0.4 mV.

For fluorescence imaging experiments, AAV-GFAP104-jRCaMP1a or AAV-GFAP104-$GRAB_{NE2m}$ virus was injected into hippocampal CA1 to measure Ca^{2+} and NE from astrocytes, respectively.

For sniffer patch experiments, primary astrocytes were prepared as previously described (24,36). Fura-2AM was loaded for 40 minutes, then washed and subjected to imaging. To induce astrocytic Ca^{2+}, 500 μM TFLLR was applied with pressure (20 lbf/in^2, 100 ms) using Picospritzer (Parker Instrument).

For 2-cell assay, source cells were prepared with transfection of *Best1*-expressing plasmids in HEK293T cells. The sensor cell was prepared as described above. A pair of one sensor and one source cell were patched, and the responsive current from sensor cells was measured under voltage clamp while the source cell was ruptured.

For permeability assay, *Best1* current was measured from the *Best1*-expressing HEK293T cell with various concentrations of substitution for chloride to D-serine. The internal solution contained 100 mM CsCl, 20 mM tetraethylammonium-Cl, 8.7 mM $CaCl_2$, 10 mM HEPES, 10 mM BAPTA, 3 mM Mg-ATP, 0.2 mM Na_2-GTP, and 0.5 mM $MgCl_2$ (pH was adjusted to 7.2 with CsOH); when D-serine was included, it replaced an equimolar amount of CsCl. Osmolarity was adjusted to 287 mosmol by adding sucrose.

For the Morris water maze (MWM), mice were tested as previously described (37). The training consisted of 4 trials/day (10-min intertrial interval) for 7 days in the hidden platform test. The training in *Best1* rescue experiments consisted of 3 trials/day. On day 8, the hidden platform was placed on the opposite quadrant for the spatial reversal learning test. For the D-serine application, D-serine (600 mg/kg) was injected intraperitoneally 20 minutes before the first trial of each day during the acquisition session. In the visible platform test, mice were trained to find a visible platform marked with a salient black tape for 2 days (4 trials/day, 10 min intertrial interval). During the test session after acquisition (day 3, trial 9), the platform was moved to an adjacent location.

Statistical analyses were performed using Prism 9 (GraphPad Software). Data were presented as mean ± SEM. No statistical method was used to predetermine sample size. Sample sizes were empirically determined based on our previous experiences.

RESULTS

Astrocytes Regulate Hippocampal NMDAR Tone Through BEST1

Astrocytic Ca^{2+} is an important signaling molecule for the release of gliotransmitters (38–40). To investigate whether astrocytic Ca^{2+} is important for the regulation of hippocampal NMDAR tone, we measured $I_{tonicNMDAR}$ (41) (Figure 1A) after astrocytic Ca^{2+} chelation with BAPTA (Figure 1B; Figure S1A). $I_{tonicNMDAR}$ was significantly reduced by astrocytic Ca^{2+} chelation (+BAPTA) compared with control (−BAPTA) (Figure 1C, D), indicating that hippocampal astrocytes can regulate NMDAR tone in a Ca^{2+}-dependent manner. Note that

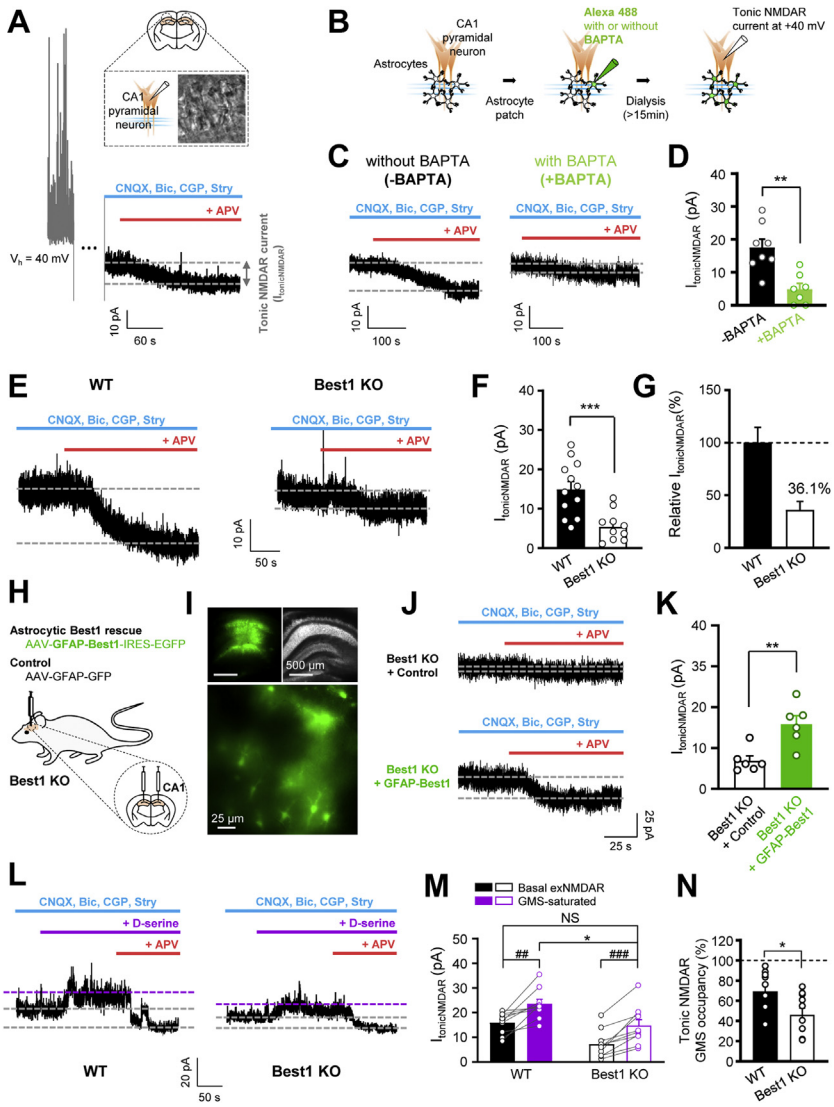

Figure 1. Astrocytes regulate hippocampal NMDAR tone through BEST1. **(A)** $I_{tonicNMDAR}$ recording in hippocampal CA1 pyramidal neuron. To isolate NMDAR-mediated current, 20 μM CNQX, 10 μM bicuculline, 10 μM CGP55845, and 10 μM strychnine were applied. A 50-μM APV-sensitive current was measured in voltage holding at +40 mV. **(B)** Astrocytic Ca^{2+} chelation with BAPTA dialysis. **(C)** Representative traces of $I_{tonicNMDAR}$ with or without BAPTA dialysis. **(D)** Summary graph of $I_{tonicNMDAR}$ with or without BAPTA dialysis. **(E–G)** Representative traces of $I_{tonicNMDAR}$ **(E)**, summary graph of $I_{tonicNMDAR}$ **(F)**, and relative $I_{tonicNMDAR}$ to WT **(G)** in WT and *Best1* knockout mice. **(H–K)** Scheme of astrocytic *Best1* rescue in CA1 of *Best1* KO mice **(H)**, images showing virus expression **(I)**, representative traces of $I_{tonicNMDAR}$ **(J)**, and summary graph of $I_{tonicNMDAR}$ in each condition **(K)**. **(L)** Application of 100 μM D-serine during $I_{tonicNMDAR}$ measurement. **(M)** Summary graph of $I_{tonicNMDAR}$ before (black) and after D-serine treatment (purple) in each condition. **(N)** Estimated tonic NMDAR GMS occupancy (%). Individual dots refer to cells. Data are represented as mean ± SEM. $^{*}p < .05$; $^{**}p < .01$; $^{***}p < .001$; Mann-Whitney *U* test **(D, K)** or unpaired *t* test **(F, M, N)**. $\#p < .05$; $\#\#p < .01$; $\#\#\#p < .001$; paired *t* test **(M)**. Bic, bicuculline; CGP, CGP55845; GMS, glycine modulatory site; KO, knockout; NMDAR, NMDA receptor; NS, not significant; Stry, strychnine; WT, wild-type.

bafilomycin A1, which blocks vesicular release, did not affect $I_{tonicNMDAR}$ (41).

Next, we examined $I_{tonicNMDAR}$ in *Best1* knockout (KO) mice (42) to investigate whether BEST1, which can release glutamate in a Ca^{2+}-dependent manner (24), regulates NMDAR tone and found that $I_{tonicNMDAR}$ was significantly reduced in *Best1* KO mice compared with wild-type mice (Figure 1E–G). The decrease in $I_{tonicNMDAR}$ in *Best1* KO mice was not due to NMDAR expression or changes in basal synaptic transmission (Figure S1B–N). To substantiate further that astrocytic BEST1 regulates NMDAR tone, BEST1 was overexpressed in hippocampal astrocytes with AAV-GFAP-*Best1*-IRES-EGFP virus (Figure 1H, I; Figure S2). *Best1* KO mice expressing BEST1 in astrocytes (GFAP-Best1) showed recovery of $I_{tonicNMDAR}$ compared with control (GFAP-GFP) (Figure 1J, K), indicating that astrocytic BEST1 mediates NMDAR tone in the hippocampus.

NMDAR tone can be attributed to both glutamate and NMDAR coagonists (i.e., D-serine or glycine), because both are required for NMDAR activation. To dissect the contribution of glutamate to NMDAR tone, the NMDAR glycine modulatory site (GMS) was saturated by 100 μM D-serine application (Figure 1L). The GMS-saturated $I_{tonicNMDAR}$ was significantly reduced in *Best1* KO mice (Figure 1M). The percentage of GMS occupancy (basal $I_{tonicNMDAR}$/GMS-saturated $I_{tonicNMDAR}$) was also significantly reduced in *Best1* KO mice. We observed a similarly reduced GMS occupancy of synaptic NMDAR (synNMDAR) in *Best1* KO, knockdown, and rescue experiments (Figure S3). Taken together, these results indicate that astrocytic BEST1 regulates the majority of NMDAR tone (63.9%) by modulating the ambient level of both glutamate and coagonists.

Next, we investigated whether $I_{tonicNMDAR}$ is mediated by extrasynaptic NMDAR (exNMDAR) or tonic activation of synNMDAR. To test this idea, only synNMDAR or both

synNMDAR and exNMDAR were inhibited by 20 μM MK-801, a use-dependent NMDAR inhibitor, and $I_{tonicNMDAR}$ was measured (Figure 2A, B). No decrease in $I_{tonicNMDAR}$ under the inhibition of synNMDAR indicated that exNMDAR rather than synNMDAR majorly mediates $I_{tonicNMDAR}$ (Figure 2C). The remaining $I_{tonicNMDAR}$ may be mediated by either the unblocked synNMDAR or the unblocked exNMDAR. These results suggest that astrocytic gliotransmission through BEST1 targets exNMDAR in addition to synNMDAR (Figure S3) (43).

D-Serine and Glutamate Are Coreleased From Astrocytes Through BEST1

Besides glutamate, to determine whether D-serine or glycine is released from astrocytes in a Ca^{2+}-dependent manner, a sniffer patch experiment was performed. TFLLR, a PAR-1 agonist, was locally applied to induce Ca^{2+}-dependent release from an astrocyte, and the sensor current was recorded from an HEK293T cell expressing either a biosensor, NMDAR (NR1-1a and chimeric NR2A[2D-S1]) for glutamate and coagonist detection, or glycine receptor (hGlyR α1 L261F) for glycine detection, but not D-serine (Figure 3A, B). We observed a significant NMDAR-sensor current but minimal glycine receptor–sensor current (Figure 3C, D), suggesting the involvement of astrocytic D-serine rather than glycine. To determine whether D-serine is released, short hairpin RNA (shRNA) for serine racemase (SR), which synthesizes D-serine, was expressed in the astrocyte (Figure 3E; Figure S4). The expression of SR shRNA reduced NMDAR-sensor current, which was restored through D-serine incubation (Figure 3E, F), indicating that astrocytes release D-serine, not glycine, to activate NMDAR. Next, we examined a possibility that D-serine directly permeates BEST1. To estimate the relative permeability of D-serine to BEST1, we recorded Ca^{2+}-activated BEST1-mediated current with serial substitutions of chloride in an internal pipette solution with equivalent concentrations of D-serine (Figure 3G). Recorded reversal potential was in between two theoretical lines of permeability (P) ratio, which are $P_{D\text{-serine}}/P_{Cl} = 1$ and $P_{D\text{-serine}}/P_{Cl} = 0$ (Figure 3H), suggesting substantial D-serine permeability to BEST1. Subsequently, we investigated whether D-serine and glutamate can be coreleased through BEST1. We employed a 2-cell sniffer patch technique, consisting of a source cell expressing BEST1 and a sensor cell expressing NR1/NR2A(2D-S1) (Figure 3I). We found a significant NMDAR-sensor current in both glutamate and D-serine for the source cell with BEST1 but not in glutamate only or with BEST1-W93C, a pore-mutant form of BEST1 (Figure 3J, K). Finally, we tested the concept of corelease of glutamate and D-serine through BEST1 in astrocytes with the sniffer patch experiment (Figure 3L). *Best1* shRNA–expressing astrocytes showed almost complete elimination of the NMDAR-sensor current, which was fully reconstituted by a coexpression of an shRNA-insensitive form of *Best1*, whereas coexpression of BEST1-W93C showed no recovery (Figure 3L–N). Taken together, these results indicate that astrocytes corelease D-serine and glutamate through BEST1 in a Ca^{2+}-dependent manner to activate adjacent NMDAR and mediate NMDAR tone in the hippocampus.

Decreased NMDAR Tone Leads to Impaired LTD in Hippocampus

Next, we examined the potential role of NMDAR tone in synaptic plasticity, with fEPSP recordings of the Schaffer collateral (SC) pathway at CA3-CA1 synapses. We found that low-frequency stimulation (LFS)–induced LTD was completely impaired in *Best1* KO mice (Figure 4A–C; Figure S5C, D), whereas the plasticity induced by high-frequency stimulation (HFS) or 10-Hz stimulation was intact (Figure 4C; Figure S5A, B). These results suggest that regulation of NMDAR tone through BEST1 is critical for the induction of LTD but not LTP. Next, to test whether the recovery of NMDAR tone with overexpression of *Best1* in astrocytes is sufficient for LTD recovery, BEST1 was overexpressed in hippocampal astrocytes of *Best1* KO mice (Figure 4D–F). Hippocampal LTD in *Best1* KO mice was restored with astrocytic BEST1 overexpression but not with control (Figure 4F). These results indicate that astrocytic

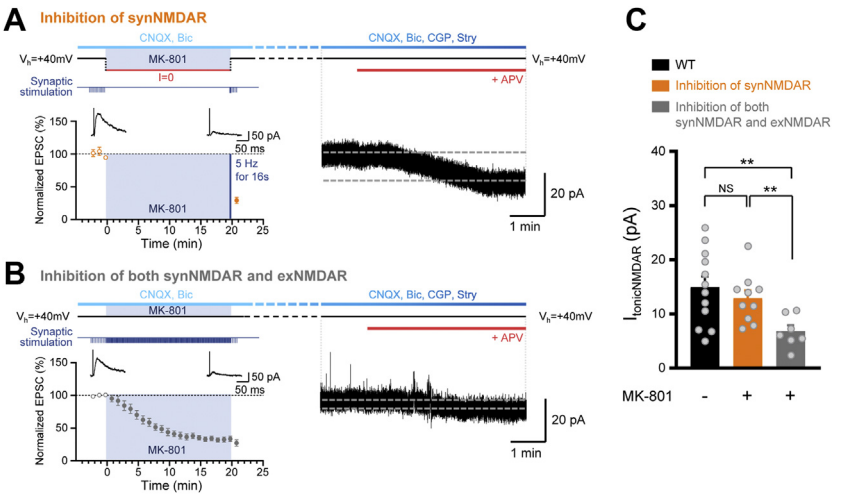

Figure 2. $I_{tonicNMDAR}$ is majorly mediated by exNMDAR rather than synNMDAR. **(A)** Upper: experimental scheme for the inhibition of synNMDAR by 20 μM MK-801. Lower: inhibition of synNMDAR current (left) and representative $I_{tonicNMDAR}$ (right). **(B)** Upper: experimental scheme for the inhibition of both synNMDAR and exNMDAR by 20 μM MK-801. Lower: inhibition of synNMDAR current (left) and representative $I_{tonicNMDAR}$ (right). Bic, bicuculline; CGP, CGP55845; EPSC, excitatory postsynaptic current; exNMDAR, extrasynaptic NMDA receptor; synNMDAR, synaptic NMDAR; Stry, strychnine; WT, wild-type.

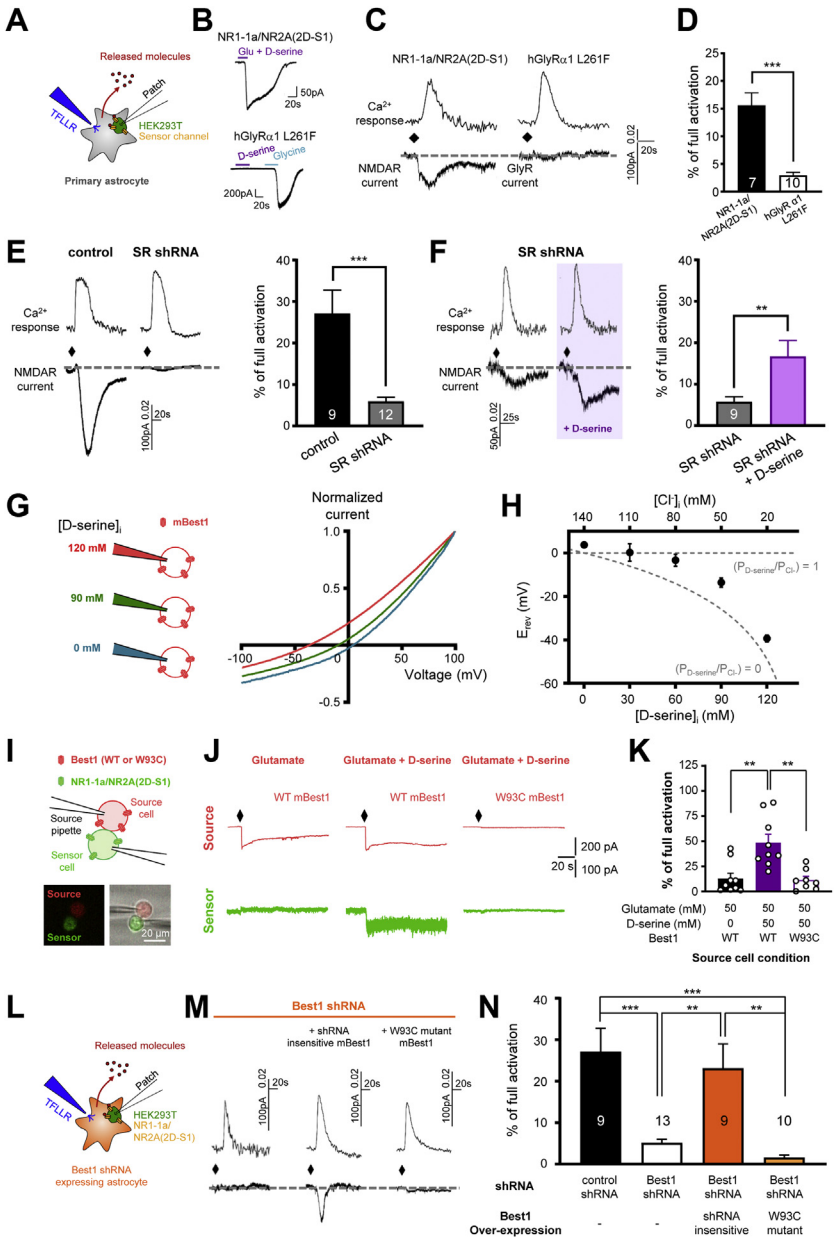

Figure 3. Astrocyte coreleases D-serine and glutamate through BEST1 to activate NMDAR. **(A)** Scheme of sniffer patch using primary astrocyte and sensor cell. **(B)** Validation of sensor channels. Upper: NR1-1a/NR2A(2D-S1)–mediated responsive current to 100 μM glutamate and 100 μM D-serine. Lower: hGlyRα1 L261F–mediated responsive current to 100 μM D-serine and 100 μM glycine, respectively. **(C)** Representative traces of Ca^{2+} response in astrocytes, and responsive sensor current from sensor cell expressing NR1-1a/NR2A(2D-S1) or hGlyRα1 L261F. **(D)** Summary graph of the peak amplitude normalized to full activation in sensor cell with NR1-1a/NR2A(2D-S1) or hGlyRα1 L261F. **(E)** Left: representative traces of SR knockdown and control. Right: summary graph of the normalized peak amplitude in each condition. **(F)** Left: representative traces of SR knockdown before and after 100 μM D-serine treatment. Right: summary graph of the normalized peak amplitude in each condition. **(G)** I-V relationship in HEK293T cell expressing BEST1 in the presence of Ca^{2+} (~4.5 μM) and varying intracellular concentrations of D-serine. **(H)** Dependence of E_{rev} (mV) on intracellular D-serine concentration. Gray dotted lines: predicted E_{rev} by the Goldman-Hodgkin-Katz equation when D-serine is as permeable as Cl^- ($P_{D\text{-serine}}/P_{Cl}$ = 1) and when D-serine is not permeable at all ($P_{D\text{-serine}}/P_{Cl}$ = 0). **(I)** Scheme of two cells assay. Source cell expressing BEST1 WT or W93C mutant. **(J)** Representative traces of currents simultaneously recorded from source (red) and sensor (green) cells. **(K)** Summary graph of the normalized peak amplitude in each condition. **(L)** Sniffer patch for astrocyte with *Best1* shRNA expression. **(M)** Representative traces of *Best1* knockdown without or with either overexpression of shRNA-insensitive form or W93C mutant form of *Best1*. **(N)** Summary graph of the normalized peak amplitude. Individual dots and numbers refer to cells. Data are represented as mean ± SEM. $^*p < .05$; $^{**}p < .01$; $^{***}p < .001$; unpaired *t* test **(D, E)**, paired *t* test **(F)**, and one-way analysis of variance with the Tukey multiple comparison test **(K, N)**. E_{rev}, current reversal potential; NMDAR, NMDA receptor; shRNA, short hairpin RNA; SR, serine racemase; WT, wild-type.

BEST1 mediates hippocampal LTD, possibly via regulation of glutamate and D-serine.

It is noteworthy that D-serine contributes to hippocampal LTD (17,44). Next, we examined the possibility that astrocytic D-serine may contribute to LTD, because D-serine can be released through BEST1. A Cre-dependent SR shRNA–expressing virus (AAV-pSico-RED SR shRNA) and a cell-specific Cre-expressing virus (AAV-GFAP-Cre for astrocytes or AAV-CaMKIIα-Cre for excitatory neurons) were coinjected into CA1 (Figure 4G). Astrocytic SR knockdown eliminated LTD, whereas neuronal SR knockdown did not (Figure 4H, I). Finally, we tested whether impaired LTD in *Best1* KO mice can be restored by increasing NMDAR tone during LTD induction. D-serine application restored impaired LTD in *Best1* KO mice (Figure 4J, K), indicating that NMDAR tone is critical for hippocampal LTD. Taken together, these results show that astrocytes are important mediators of NMDAR tone and hippocampal LTD.

Norepinephrine Induces NMDAR Tone and LTD in Hippocampus

NE activates astrocytic Ca^{2+} through α1-AR (26) (Figure S6A–D) and induces α1-AR–dependent LTD (27). Next, we examined whether NE-LTD is dependent on NMDAR tone. A 200-μM NE application induced a significant $I_{tonicNMDAR}$, which was

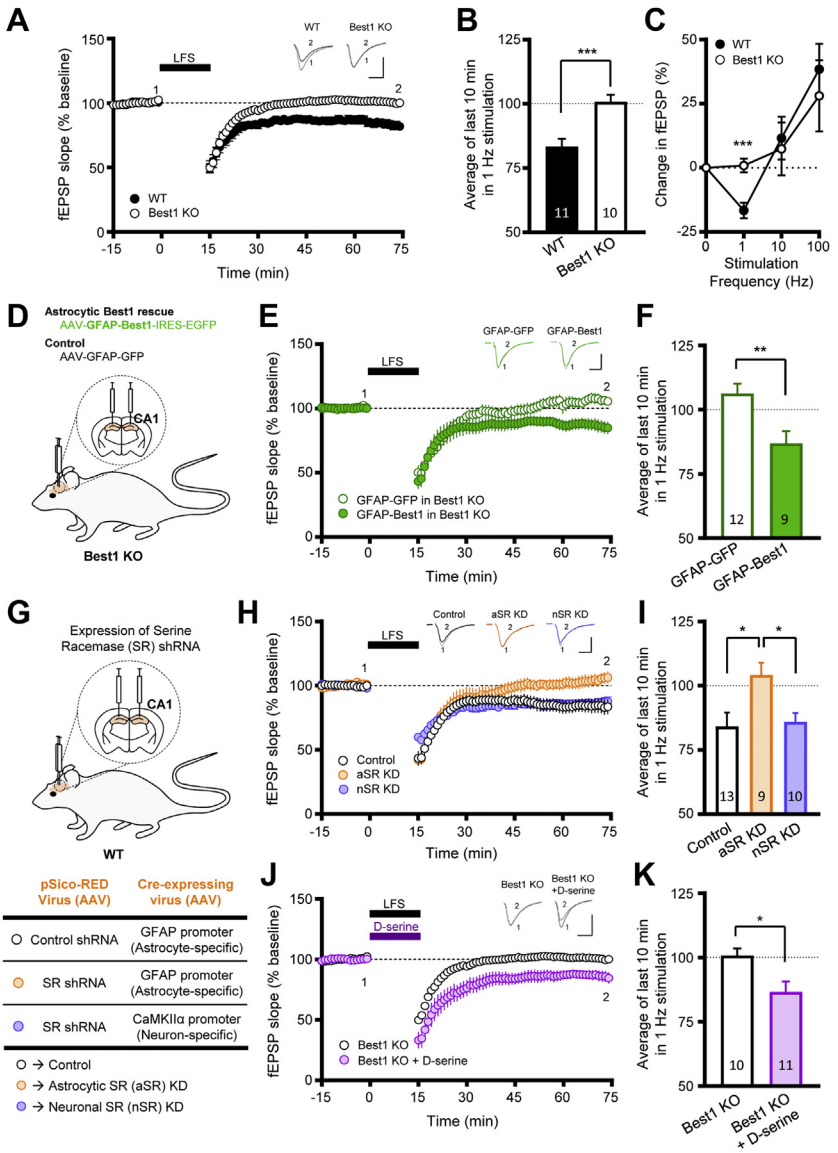

Figure 4. Astrocytic regulation of NMDAR tone through BEST1 is important for LTD induction. **(A)** LFS (900 stim. at 1 Hz)–induced LTD in WT and *Best1* KO mice. **(B)** Summary graph of LFS-induced LTD in each condition. **(C)** Bienenstock–Cooper–Munro curve of synaptic plasticity in each condition. **(D)** Scheme of CA1 astrocyte-specific *Best1* rescue in *Best1* KO mice. **(E, F)** LFS-induced LTD **(E)** and summary graph **(F)** in CA1 astrocyte-specific *Best1* rescue from *Best1* KO mice. **(G)** Scheme of cell type–specific SR KD. **(H, I)** LFS-induced LTD **(H)** and summary graph **(I)** in cell type–specific SR KD experiment. **(J, K)** LTD induction in *Best1* KO mice with 20 μM D-serine application during LFS **(J)** and summary graph **(K)**. Numbers in the graphs refer to hippocampal slices. Scale bar: 1 mV, 10 ms. Data are represented as mean ± SEM. $^{*}p < .05$; $^{**}p < .01$; $^{***}p < .001$; unpaired *t* test **(B, C, F, K)**, and one-way analysis of variance with the Tukey multiple comparison test **(I)**. fEPSP, field excitatory postsynaptic potential; KD, knockdown; KO, knockout; LFS, low-frequency stimulation; LTD, long-term depression; NMDAR, NMDA receptor; shRNA, short hairpin RNA; SR, serine racemase; WT, wild-type.

blocked by APV (Figure 5A–C). The 200-μM NE-induced $I_{tonicNMDAR}$ was almost completely eliminated in *Best1* KO mice and significantly restored by D-serine (Figure 5B, C), suggesting that NE increases NMDAR tone through BEST1 in the hippocampus. Then, NE-LTD was examined to determine its correlation with NMDAR tone. We found that NE-LTD was blocked by APV in wild-type mice, absent in *Best1* KO mice, and restored by D-serine in *Best1* KO mice (Figure 5D–G). Taken together, these results indicate that NE-LTD is induced by NMDAR tone mediated by *Best1*.

HFS-Induced Norepinephrine Release Mediates Heterosynaptic LTD

Most of the NE in the brain is supplied by fiber projections from the LC, and SC stimulation or glutamate application has been shown to induce NE release (45–47). We further investigated the effect of SC stimulation on release of NE-targeting hippocampal astrocytes. Through SC stimulation in which $GRAB_{NE2m}$, a GPCR-based NE fluorescence sensor, was specifically expressed in astrocytes, we found that NE release was increased in an intensity- and frequency-dependent manner (Figure 6A–G). These results suggest that presynaptic CA3 activation can induce NE release, possibly through presynaptic AMPA receptors (Figure S6E–H).

The fact that NE was significantly released by HFS led to the hypothesis that NE-LTD caused by NMDAR tone may occur during HFS. Because HFS induces LTD at heterosynaptic (unstimulated) synapses while inducing LTP (48), we examined whether heterosynaptic LTD shares a similar molecular mechanism with NE-LTD. After establishing two independent

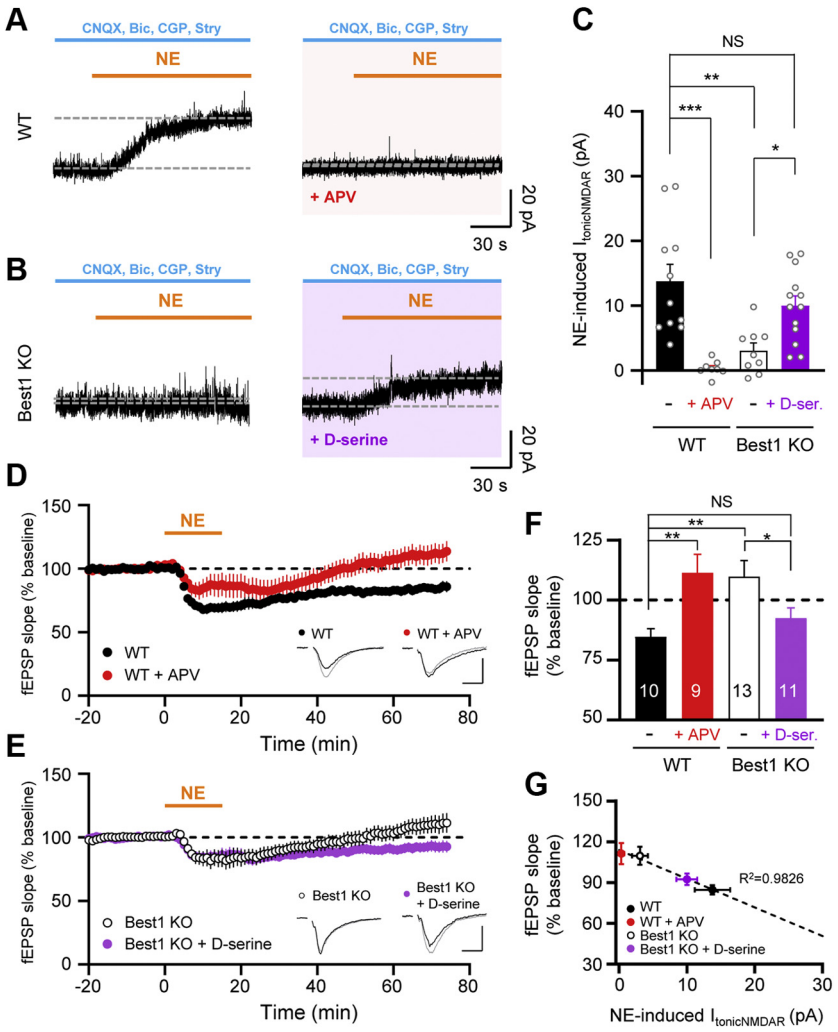

Figure 5. NE induces NMDAR tone increase and NE-LTD. **(A)** Representative traces of NE-induced $I_{tonicNMDAR}$ in WT without or with APV. **(B)** Representative traces of NE-induced $I_{tonicNMDAR}$ in *Best1* KO mice without or with 100 μM D-serine. **(C)** Summary graph of NE-induced $I_{tonicNMDAR}$ in each condition. **(D)** NE-induced LTD in WT without or with APV. **(E)** NE-induced LTD in *Best1* KO mice without or with 100 μM D-serine. **(F)** Summary graph of 200-μM NE-induced LTD in each condition. **(G)** Correlation graph for NE-induced $I_{tonicNMDAR}$ and NE-induced fEPSP slope change. Numbers in the graphs refer to hippocampal slices **(F)**, and individual dots refer to cells. Scale bar: 1 mV, 10 ms. Data are represented as mean ± SEM. $^{*}p < .05$; $^{**}p < .01$; $^{***}p < .001$; one-way analysis of variance with the Tukey multiple comparisons test **(C)** and unpaired *t* test **(F)**. Bic, bicuculline; CGP, CGP55845; fEPSP, field excitatory postsynaptic potential; KO, knockout; LTD, long-term depression; NE, norepinephrine; NMDAR, NMDA receptor; NS, not significant; Stry, strychnine; WT, wild-type.

stimuli (Figure 6H, I), heterosynaptic LTD was induced by HFS (Figure 6J, K). Prazosin blocked heterosynaptic LTD but not homosynaptic LTP (Figure 6J, K), indicating that α1-AR is necessary for heterosynaptic LTD. Heterosynaptic LTD, but not homosynaptic LTP, was impaired in *Best1* KO mice and restored by an enhancement of NMDAR tone with D-serine (Figure 6J–M). Taken together, these results indicate that NE-α1-AR mediates heterosynaptic LTD through NMDAR tone.

Repotentiation Is Impaired in *Best1* KO Mice

Heterosynaptic plasticity has been proposed to enable further changes in synaptic plasticity, i.e., metaplasticity (32). Next, we examined whether a decrease in heterosynaptic LTD in *Best1* KO mice affects metaplasticity, using a bidirectional modification protocol (49), consisting of first HFS, LFS, and second HFS (Figure 7A). We found that repotentiation, but not depotentiation, was significantly impaired in *Best1* KO mice (Figure 7A, B; Figure S7). To test whether impaired repotentiation in *Best1* KO mice can be restored by an enhancement of NMDAR tone, D-serine was applied during the first HFS (orange), LFS (green), or second HFS window (blue) (Figure 7C–F). We found that repotentiation was restored by D-serine treatment during the first HFS window but not the LFS or second HFS windows (Figure 7C–F). These results suggest that NMDAR tone during initial HFS required for heterosynaptic LTD is critical for subsequent repotentiation and metaplasticity.

Astrocytic BEST1 and NMDAR Tone Regulation Are the Keys for Cognitive Flexibility and Flexible Memory Formation

To investigate the role of BEST1-mediated NMDAR tone in learning and memory, we performed various hippocampus-dependent memory tasks, such as the MWM, passive avoidance test, and contextual fear conditioning test, with *Best1* KO mice (Figure 8A; Figure S8). We found no difference in memory acquisition during the MWM, passive avoidance test, and contextual fear conditioning, vision, and locomotion

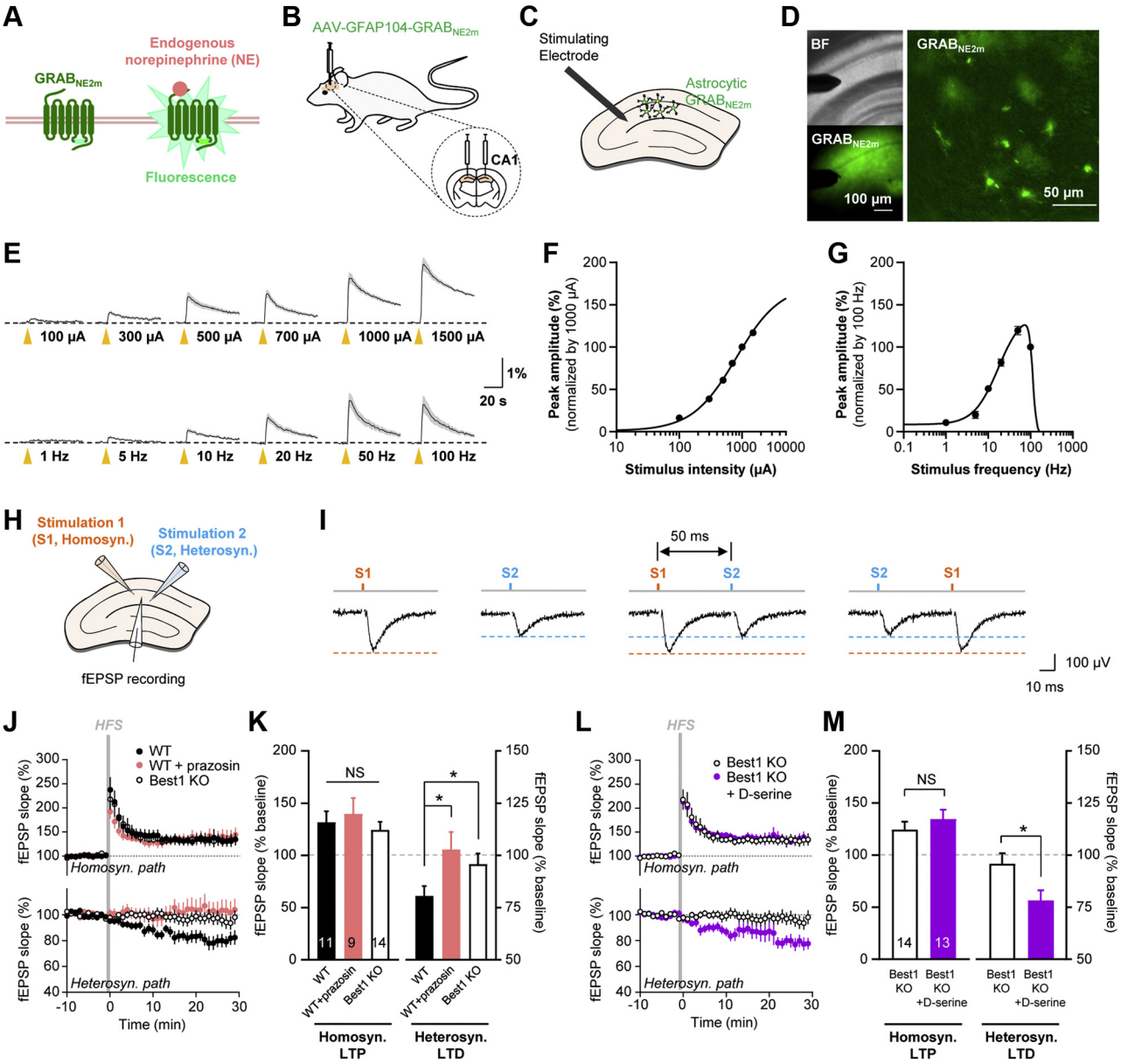

Figure 6. Local NE release mediates heterosynaptic LTD through NMDAR tone. **(A)** GRAB$_{NE2m}$, a fluorescent sensor for NE. **(B)** Astrocytic expression of GRAB$_{NE2m}$ with AAV-GFAP104-GRAB$_{NE2m}$. **(C)** Scheme of evoked NE release by Schaffer collateral stimulation. **(D)** Images of GRAB$_{NE2m}$ in hippocampal CA1. **(E)** Representative traces of GRAB$_{NE2m}$ response by the various stimulation. **(F)** Stimulus intensity-GRAB$_{NE2m}$ response curve (at 20 Hz). **(G)** Stimulus frequency-GRAB$_{NE2m}$ response curve (at 500 μA). **(H)** Scheme of simultaneous homosynaptic (S1, orange) and heterosynaptic (S2, blue) recordings. **(I)** Lack of heterosynaptic facilitation with 50-ms interval. **(J)** Homosynaptic and heterosynaptic changes by HFS in WT, WT with 10 μM prazosin, and *Best1* KO mice. **(K)** Summary graph of fEPSP changes in **(J)**. **(L)** Homosynaptic and heterosynaptic changes by HFS in *Best1* KO mice and *Best1* KO mice with 100 μM D-serine. **(M)** Summary graph of fEPSP changes in **(L)**. Numbers in the graphs refer to hippocampal slices. Data are represented as mean ± SEM. $^{*}p < .05$; $^{**}p < .01$; $^{***}p < .001$; unpaired *t* test **(K, M)**. fEPSP, field excitatory postsynaptic potential; Heterosyn., heterosynaptic; HFS, high-frequency stimulation; Homosyn., homosynaptic; KO, knockout; LTD, long-term depression; NE, norepinephrine; NMDAR, NMDA receptor; NS, not significant; WT, wild-type.

(Figure 8A–E; Figure S8). Contrarily, *Best1* KO mice showed impaired reversal learning in the MWM (Figure 8B, C). This impaired reversal learning was sufficiently recovered by astrocytic BEST1 overexpression (Figure 8F), indicating that astrocytic BEST1 is critical for cognitive flexibility.

Finally, we hypothesized that NMDAR tone during initial memory acquisition contributes to reversal learning and flexible memory formation, because it enables heterosynaptic LTD and further repotentiation. To test this hypothesis, we enhanced NMDAR tone by administering D-serine only during

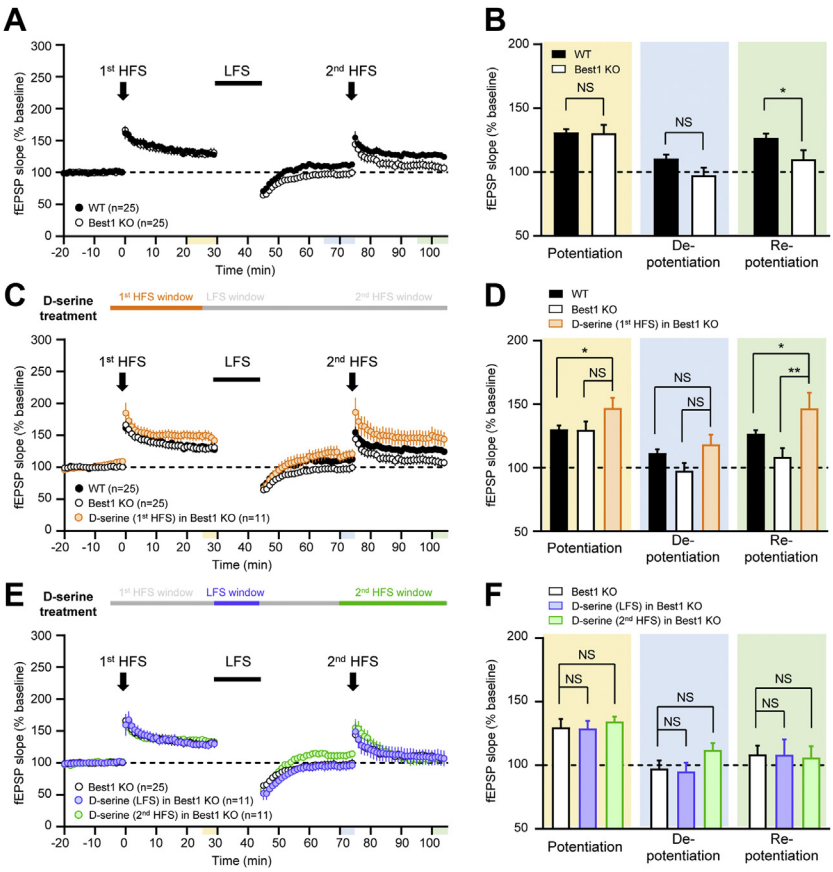

Figure 7. NMDAR tone during first potentiation promotes repotentiation. **(A, B)** Time course of the normalized fEPSP slope changes **(A)** and summary graph **(B)** of first HFS-induced potentiation, LFS-induced depotentiation, and second HFS-induced repotentiation in WT and *Best1* KO mice. **(C)** NMDAR tone enhancement during first HFS window in *Best1* KO mice by 20 μM D-serine treatment. **(D)** Summary graph of results from **(C)**. **(E)** NMDAR tone enhancement during LFS or second HFS window in *Best1* KO mice by 20 μM D-serine treatment. **(F)** Summary graph of the results from **(E)**. Data are represented as mean ± SEM. $^{*}p < .05$; $^{**}p < .01$; $^{***}p < .001$; unpaired *t* test **(B, D, F)**. fEPSP, field excitatory postsynaptic potential; HFS, high-frequency stimulation; LFS, low-frequency stimulation; KO, knockout; NMDAR, NMDA receptor; NS, not significant; WT, wild-type.

initial memory acquisition and then examined reversal learning (Figure 8G–L). Enhanced NMDAR tone during initial memory acquisition restored reversal learning in *Best1* KO mice (Figure 8K, L), indicating that NMDAR tone during initial memory acquisition is critical for the formation of flexible memory.

Altogether, these findings establish that astrocytes render memory flexible through BEST1 by regulating NMDAR tone during initial memory acquisition (Figure S9).

DISCUSSION

We have presented that astrocytes are critically involved in reversal learning and flexible memory formation. Astrocytes achieve this unique function by coreleasing D-serine and glutamate through BEST1 on activation of the NE–α1-AR pathway, leading to an enhanced NMDAR tone and heterosynaptic LTD during initial memory acquisition. Our study provides a comprehensive understanding of how NE, NMDAR tone, and memory formation are associated.

Astrocyte as a Regulator of NMDAR Tone

It has been proposed that astrocytes mediate NMDAR tone in the hippocampus (41). However, this concept of astrocytic contribution to NMDAR tone has been challenged by the investigation on IP_3 receptor type 2 (IP3R2) KO, showing no difference in hippocampal NMDAR tone (50). Contrary to this conflicting observation, we found that astrocytes majorly contribute to hippocampal NMDAR tone in a Ca^{2+}-dependent manner through BEST1. Our results raise the possibility that IP3R2-mediated Ca^{2+} may not be necessary for the activation of BEST1, and other calcium sources [e.g., IP3R2-independent Ca^{2+} from endoplasmic reticulum (51), endoplasmic reticulum–Ca^{2+}-independent Ca^{2+} (52–54)] should be investigated in future studies.

In this study, we have identified D-serine as a novel permeant molecule passing through BEST1 and demonstrated that astrocytic BEST1 is an ideal regulator of NMDAR tone by releasing both glutamate and D-serine in the hippocampus. Our study directly addresses the recent controversy over the origin of D-serine (19,20) and provides answers with astrocyte-specific manipulations. Although SR has been reported to be expressed in both astrocytes (19) and neurons (20), neuronal synthesis and release of D-serine may not contribute to the D-serine content in the hippocampus (55) and hippocampal LTD (56). We have found that BEST1-mediated D-serine release from astrocytes is particularly important for hippocampal LTD, showing a critical role of D-serine for LTD (17). In contrast, BEST1-mediated D-serine release is not required for LTP, suggesting an alternative molecular (57,58) or cellular mechanism (55,59) of release of D-serine or glycine or both for LTP

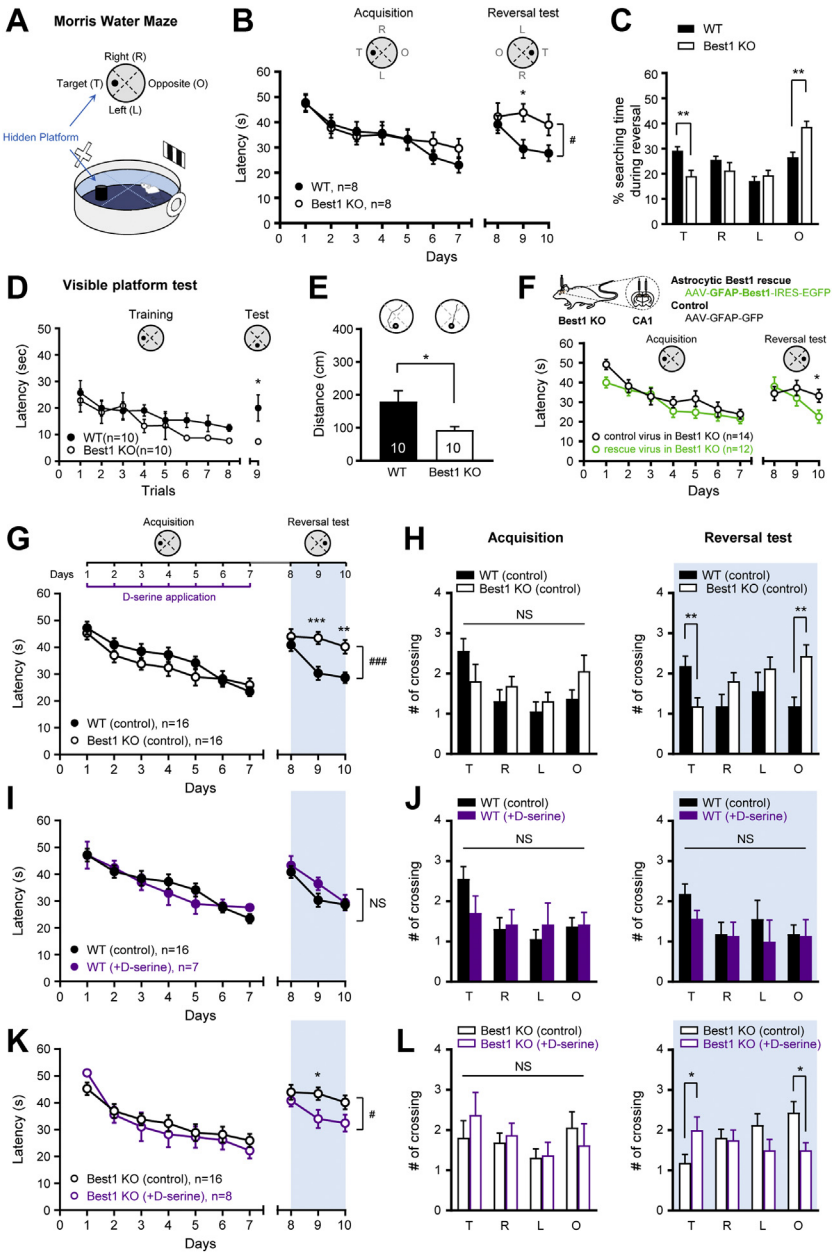

Figure 8. NMDAR tone is critical for formation of flexible memory. **(A)** Scheme of Morris water maze. **(B)** Escape latency of WT and *Best1* KO in acquisition and reversal test session. **(C)** Searching time of WT and *Best1* KO mice during reversal test in each quadrant. **(D, E)** Escape latency **(D)** and moved distance **(E)** of WT and *Best1* KO mice in visible platform test. **(F)** Escape latency of *Best1* KO mice with the rescue of astrocytic BEST1, in acquisition and reversal test session during hidden platform test. **(G–L)** Application of saline or D-serine (600 mg/kg, intraperitoneal injection) in each day of acquisition session. **(G, I, K)** Escape latency of WT and *Best1* KO mice with application of saline or D-serine. **(H, J, L)** Left: number of crossing to each quadrant in each condition during acquisition session. Right: number of crossing to each quadrant in each condition during reversal test session. Numbers in the graphs refer to animals. Data are represented as mean ± SEM. $^{*}p < .05$; $^{**}p < .01$; $^{***}p < .001$; two-way analysis of variance with Fisher's least significant difference **(B, D, F)** and unpaired *t* test **(C, E, G–L)**. $^{\#}p < .05$; $\#\#p < .01$; $\#\#\#p < .001$; two-way repeated measures analysis of variance (genotype or treatment) **(B, G, I, K)**. KO, knockout; NMDAR, NMDA receptor; NS, not significant; WT, wild-type.

induction. Still, BEST1-mediated glutamate can lower the threshold for LTP (43) on PAR1 activation, so further researches on other types of LTP (e.g., late LTP) and learning paradigm are needed. In addition, more detailed molecular mechanisms by which astrocytes induce NMDAR-dependent LTD [e.g., Ca^{2+} influx through ionotropic NMDAR (60) or metabotropic signaling through non-ionotropic NMDAR (61)] need to be further established.

It is interesting to note that D-serine administration alone was able to restore the impairments in *Best1* KO mice. We estimated that only 37.4% of glutamate was reduced in *Best1* KO mice, indicating that there is an additional mechanism for remaining ambient glutamate in *Best1* KO mice. Additional possible mechanisms for astrocytic glutamate release include xCT (62), vesicular glutamate release (63), or volume-regulated anion channel (64,65). It should be noted that an xCT inhibitor, sulfasalazine, reduced $I_{tonicNMDAR}$ by 66.8% (Figure S10), indicating the predominant contribution of xCT to ambient glutamate. Owing to the additional mechanism of remaining tonic glutamate in *Best1* KO mice, only D-serine administration was sufficient to show the recovery effects. Whether the various mechanisms of astrocytes that release glutamate or D-

serine work cooperatively (66) and how astrocytic uptake through transporters contribute to NMDAR tone have been poorly established. In particular, the clearance of NMDAR tone through transporters (e.g., GLT-1 or GLAST) may be important to prevent overspread of NMDAR tone and heterosynaptic LTD. These interesting topics await future investigation. Furthermore, the concept of astrocytic regulation of NMDAR tone should not be limited to the hippocampus but should be applicable to other brain regions (e.g., cortex) (66,67).

Local Norepinephrine Release Mediates Heterosynaptic LTD via Astrocytic Regulation of NMDAR Tone

In this study, we found that SC stimulation induces NE release by activating presynaptic AMPA receptors (68) at the LC terminals of so-called en passant varicosities (69), forming axoaxonic synapses. These results are consistent with previous reports that glutamate induces local NE release (45,46) and supports the hypothesis of local control of NE release (70). HFS-induced NE release induces heterosynaptic LTD through α1-AR, which is a key receptor in astrocytes for NE-LTD induction. These results suggest that astrocytes play an essential role in heterosynaptic LTD, which is consistent with previous reports (31,71). Given that one CA1 astrocyte is in contact with about 140,000 synapses from numerous neurons (72), it is plausible to consider one astrocyte to mediate heterosynaptic LTD at unstimulated synapses while stimulated synapses are potentiated. Thus, astrocytes provide a unique structural medium for a simultaneous dynamic control of multiple synapses from both stimulated and unstimulated neurons, mediating various forms of homeostatic plasticity and metaplasticity.

Heterosynaptic LTD Can Determine Flexibility of Memory

Cognitive flexibility has long been explained only by homosynaptic LTD (9,73,74). However, conflicting reports suggest alternative mechanisms (15,16). In this study, we suggest that heterosynaptic LTD accompanying homosynaptic LTP contributes to cognitive flexibility. One functional difference between homosynaptic and heterosynaptic LTD in cognitive flexibility is that homosynaptic LTD occurs during memory modification (74), whereas heterosynaptic LTD occurs during memory acquisition. The results that D-serine administration during LTP induction or during initial memory acquisition restored heterosynaptic LTD and reversal learning in *Best1* KO mice support the importance of heterosynaptic LTD for cognitive flexibility. We construe these results as when the initial memory is formed, the memory that accompanies heterosynaptic LTD becomes a flexible memory, and the memory that does not accompany becomes an inflexible memory. This idea proposes that less flexible memory can be formed during memory acquisition under certain conditions in which heterosynaptic LTD is impaired. Consistently, administration of prazosin, which blocks heterosynaptic LTD, has been reported to interfere with subsequent extinction learning (75,76). Decreased cognitive flexibility in aging (77) and AD (5) is possibly associated with impaired heterosynaptic LTD due to decreased glutamate-induced NE release (78) or damaged LC (79), respectively. It would be interesting to investigate whether heterosynaptic LTD is impaired in aging, AD, and other brain diseases in which cognitive flexibility decreases (e.g., autism spectrum disorder, schizophrenia). Altogether, these findings extend our current knowledge of cognitive flexibility beyond homosynaptic plasticity to heterosynaptic plasticity, metaplasticity, and flexible memory.

In conclusion, we established that astrocytes play a crucial role in flexible memory formation by enabling heterosynaptic LTD at unstimulated synapses to facilitate the formation of new memories when environment and circumstances change. These findings broaden our understanding of astrocytic roles in memory formation and provide potential therapeutic targets for impaired cognitive flexibility in various psychiatric diseases.

ACKNOWLEDGMENTS AND DISCLOSURES

This study was supported by the Creative Research Initiative Program funded by the National Research Foundation of Korea (Grant No. 2015R1A3A2066619 [to CJL]), Korea Institute of Science and Technology Institutional Program (Project No. 2E26860 [to CJL]), and Institute for Basic Science, Center for Cognition and Sociality (Grant No. IBSR001-D2 [to CJL]).

WK, YEC, JL, MGP, HK, JW, and HC performed electrophysiological experiments. WK, MP, and HSS performed behavioral experiments. WK and SK performed slice imaging experiments. WK, MGP, MS, JJ, S-JO, SEL, JH, and JF performed molecular experiments. YL, HR, JC, and CJL gave technical support and conceptual advice. CJL supervised the project. WK and CJL wrote the manuscript. WK and CJL revised the manuscript.

We thank Dr. Yuriy Pankratov for proofreading the manuscript.

A previous version of this article was published as a preprint on bioRxiv: https://www.biorxiv.org/content/10.1101/2021.03.25.436945v1.

The authors report no biomedical financial interests or potential conflicts of interest.

ARTICLE INFORMATION

From the Department of Neuroscience (WK, MP, YEC, JW, CJL), Division of BioMedical Science & Technology, Korea Institute of Science and Technology School, Korea University of Science and Technology; KU-KIST Graduate School of Converging Science and Technology (MGP, SK, MS, CJL), Korea University; Convergence Research Center for Diagnosis, Treatment and Care System of Dementia (S-JO), Korea Institute of Science and Technology; Virus Facility (SEL), Research Animal Resource Center, Korea Institute of Science and Technology; Center for Functional Connectomics (WK, YEC, JL, SK, JW, HC, JH) and Center for Neuroscience (MP, HSS, S-JO, HR), Brain Science Institute, Korea Institute of Science and Technology; and Brain and Cognitive Science (JC), Scranton College, Ewha Womans University, Seoul; Center for Cognition and Sociality (WK, MGP, SK, MS, JJ, HK, HC, CJL), Institute for Basic Science; IBS School (JJ, HK, CJL), Korea University of Science and Technology, Daejeon, South Korea; and State Key Laboratory of Membrane Biology (JF, YL), Peking University School of Life Sciences, Beijing, China.

Address correspondence to C. Justin Lee, Ph.D., at cjl@ibs.re.kr.

Received May 20, 2021; revised Oct 7, 2021; accepted Oct 8, 2021.

Supplementary material cited in this article is available online at https://doi.org/10.1016/j.biopsych.2021.10.012.

REFERENCES

1. Tello-Ramos MC, Branch CL, Kozlovsky DY, Pitera AM, Pravosudov VV (2019): Spatial memory and cognitive flexibility trade-offs: To be or not to be flexible, that is the question. Anim Behav 147:129–136.
2. D'Cruz AM, Ragozzino ME, Mosconi MW, Shrestha S, Cook EH, Sweeney JA (2013): Reduced behavioral flexibility in autism spectrum disorders. Neuropsychology 27:152–160.

3. Wobrock T, Ecker UKH, Scherk H, Schneider-Axmann T, Falkai P, Gruber O (2009): Cognitive impairment of executive function as a core symptom of schizophrenia. World J Biol Psychiatry 10:442–451.
4. Etienne V, Marin-Lamellet C, Laurent B (2013): Mental flexibility impairment in drivers with early Alzheimer's disease: A simulator-based study. IATSS Res 37:16–20.
5. Guarino A, Favieri F, Boncompagni I, Agostini F, Cantone M, Casagrande M (2019): Executive functions in Alzheimer disease: A systematic review. Front Aging Neurosci 10:437.
6. Lee G, Zhou Y (2019): NMDAR hypofunction animal models of schizophrenia. Front Mol Neurosci 12:185.
7. Gandal MJ, Anderson RL, Billingslea EN, Carlson GC, Roberts TPL, Siegel SJ (2012): Mice with reduced NMDA receptor expression: More consistent with autism than schizophrenia? Genes Brain Behav 11:740–750.
8. Huang YJ, Lin CH, Lane HY, Tsai GE (2012): NMDA neurotransmission dysfunction in behavioral and psychological symptoms of Alzheimer's disease. Curr Neuropharmacol 10:272–285.
9. Nicholls RE, Alarcon JM, Malleret G, Carroll RC, Grody M, Vronskaya S, Kandel ER (2008): Transgenic mice lacking NMDAR-dependent LTD exhibit deficits in behavioral flexibility. Neuron 58:104–117.
10. Li J, Chai A, Wang L, Ma Y, Wu Z, Yu H, *et al.* (2015): Synaptic P-Rex1 signaling regulates hippocampal long-term depression and autism-like social behavior. Proc Natl Acad Sci U S A 112:E6964–E6972.
11. Morice E, Billard JM, Denis C, Mathieu F, Betancur C, Epelbaum J, *et al.* (2007): Parallel loss of hippocampal LTD and cognitive flexibility in a genetic model of hyperdopaminergia. Neuropsychopharmacology 32:2108–2116.
12. Duffy S, Labrie V, Roder JC (2008): D-serine augments NMDA-NR2B receptor-dependent hippocampal long-term depression and spatial reversal learning. Neuropsychopharmacology 33:1004–1018.
13. Izquierdo A, Brigman JL, Radke AK, Rudebeck PH, Holmes A (2017): The neural basis of reversal learning: An updated perspective. Neuroscience 345:12–26.
14. Dudek SM, Bear MF (1992): Homosynaptic long-term depression in area CA1 of hippocampus and effects of N-methyl-D-aspartate receptor blockade. Proc Natl Acad Sci U S A 89:4363–4367.
15. Rutten K, Wallace TL, Works M, Prickaerts J, Blokland A, Novak TJ, *et al.* (2011): Enhanced long-term depression and impaired reversal learning in phosphodiesterase 4B-knockout (PDE4B−/−) mice. Neuropharmacology 61:138–147.
16. Zhang M, Wang H (2013): Mice overexpressing type 1 adenylyl cyclase show enhanced spatial memory flexibility in the absence of intact synaptic long-term depression. Learn Mem 20:352–357.
17. Zhang Z, Gong N, Wang W, Xu L, Xu TL (2008): Bell-shaped D-serine actions on hippocampal long-term depression and spatial memory retrieval. Cereb Cortex 18:2391–2401.
18. Labrie V, Duffy S, Wang W, Barger SW, Baker GB, Roder JC (2008): Genetic inactivation of D-amino acid oxidase enhances extinction and reversal learning in mice. Learn Mem 16:28–37.
19. Papouin T, Henneberger C, Rusakov DA, Oliet SHR (2017): Astroglial versus neuronal D-serine: Fact checking. Trends Neurosci 40:517–520.
20. Wolosker H, Balu DT, Coyle JT (2017): Astroglial versus neuronal D-serine: Check your controls. Trends Neurosci 40:520–522.
21. Shen W, Nikolic L, Meunier C, Pfrieger F, Audinat E (2017): An autocrine purinergic signaling controls astrocyte-induced neuronal excitation. Sci Rep 7:11280.
22. Navarrete M, Cuartero MI, Palenzuela R, Draffin JE, Konomi A, Serra I, *et al.* (2019): Astrocytic p38α MAPK drives NMDA receptor-dependent long-term depression and modulates long-term memory. Nat Commun 10:2968.
23. Oh SJ, Lee CJ (2017): Distribution and function of the bestrophin-1 (Best1) channel in the brain. Exp Neurobiol 26:113–121.
24. Woo DH, Han KS, Shim JW, Yoon BE, Kim E, Bae JY, *et al.* (2012): TREK-1 and Best1 channels mediate fast and slow glutamate release in astrocytes upon GPCR activation. Cell 151:25–40.
25. Park H, Han KS, Oh SJ, Jo S, Woo J, Yoon BE, Lee CJ (2013): High glutamate permeability and distal localization of Best1 channel in CA1 hippocampal astrocyte. Mol Brain 6:54.
26. Duffy S, MacVicar BA (1995): Adrenergic calcium signaling in astrocyte networks within the hippocampal slice. J Neurosci 15:5535–5550.
27. Scheiderer CL, Dobrunz LE, McMahon LL (2004): Novel form of long-term synaptic depression in rat hippocampus induced by activation of alpha 1 adrenergic receptors. J Neurophysiol 91:1071–1077.
28. Lee HK, Kameyama K, Huganir RL, Bear MF (1998): NMDA induces long-term synaptic depression and dephosphorylation of the GluR1 subunit of AMPA receptors in hippocampus. Neuron 21:1151–1162.
29. Rorabaugh JM, Chalermpalanupap T, Botz-Zapp CA, Fu VM, Lembeck NA, Cohen RM, Weinshenker D (2017): Chemogenetic locus coeruleus activation restores reversal learning in a rat model of Alzheimer's disease. Brain 140:3023–3038.
30. Pinto-Duarte A, Roberts AJ, Ouyang K, Sejnowski TJ (2019): Impairments in remote memory caused by the lack of type 2 IP3 receptors. Glia 67:1976–1989.
31. Chen J, Tan Z, Zeng L, Zhang X, He Y, Gao W, *et al.* (2013): Heterosynaptic long-term depression mediated by ATP released from astrocytes. Glia 61:178–191.
32. Chen JY, Lonjers P, Lee C, Chistiakova M, Volgushev M, Bazhenov M (2013): Heterosynaptic plasticity prevents runaway synaptic dynamics. J Neurosci 33:15915–15929.
33. Abraham WC, Bear MF (1996): Metaplasticity: The plasticity of synaptic plasticity. Trends Neurosci 19:126–130.
34. Hulme SR, Jones OD, Raymond CR, Sah P, Abraham WC (2013): Mechanisms of heterosynaptic metaplasticity. Philos Trans R Soc Lond B Biol Sci 369:20130148.
35. Kwak H, Koh W, Kim S, Song K, Shin JI, Lee JM, *et al.* (2020): Astrocytes control sensory acuity via tonic inhibition in the thalamus. Neuron 108:691–706.e10.
36. Lee CJ, Mannaioni G, Yuan H, Woo DH, Gingrich MB, Traynelis SF (2007): Astrocytic control of synaptic NMDA receptors. J Physiol 581:1057–1081.
37. Park M, Kim CH, Jo S, Kim EJ, Rhim H, Lee CJ, *et al.* (2015): Chronic stress alters spatial representation and bursting patterns of place cells in behaving mice. Sci Rep 5:16235.
38. Sahlender DA, Savtchouk I, Volterra A (2014): What do we know about gliotransmitter release from astrocytes? Philos Trans R Soc Lond B Biol Sci 369:20130592.
39. Semyanov A, Henneberger C, Agarwal A (2020): Making sense of astrocytic calcium signals—From acquisition to interpretation. Nat Rev Neurosci 21:551–564.
40. Lalo U, Koh W, Lee CJ, Pankratov Y (2021): The tripartite glutamatergic synapse. Neuropharmacology 199:108758.
41. Le Meur K, Galante M, Angulo MC, Audinat E (2007): Tonic activation of NMDA receptors by ambient glutamate of non-synaptic origin in the rat hippocampus. J Physiol 580:373–383.
42. Marmorstein LY, Wu J, McLaughlin P, Yocom J, Karl MO, Neussert R, *et al.* (2006): The light peak of the electroretinogram is dependent on voltage-gated calcium channels and antagonized by bestrophin (best-1). J Gen Physiol 127:577–589.
43. Park H, Han KS, Seo J, Lee J, Dravid SM, Woo J, *et al.* (2015): Channel-mediated astrocytic glutamate modulates hippocampal synaptic plasticity by activating postsynaptic NMDA receptors [published correction appears in Mol Brain 2021; 14:103]. Mol Brain 8:7.
44. Papouin T, Ladépêche L, Ruel J, Sacchi S, Labasque M, Hanini M, *et al.* (2012): Synaptic and extrasynaptic NMDA receptors are gated by different endogenous coagonists. Cell 150:633–646.
45. Malva JO, Carvalho AP, Carvalho CM (1994): Modulation of dopamine and noradrenaline release and of intracellular Ca2+ concentration by presynaptic glutamate receptors in hippocampus. Br J Pharmacol 113:1439–1447.
46. Howells FM, Russell VA (2008): Glutamate-stimulated release of norepinephrine in hippocampal slices of animal models of attention-deficit/hyperactivity disorder (spontaneously hypertensive rat) and depression/anxiety-like behaviours (Wistar-Kyoto rat). Brain Res 1200:107–115.

47. Feng J, Zhang C, Lischinsky JE, Jing M, Zhou J, Wang H, *et al.* (2019): A genetically encoded fluorescent sensor for rapid and specific in vivo detection of norepinephrine. Neuron 102:745–761.e8.
48. Scanziani M, Nicoll RA, Malenka RC (1996): Heterosynaptic long-term depression in the hippocampus. J Physiol Paris 90:165–166.
49. Dudek SM, Bear MF (1993): Bidirectional long-term modification of synaptic effectiveness in the adult and immature hippocampus. J Neurosci 13:2910–2918.
50. Petravicz J, Fiacco TA, McCarthy KD (2008): Loss of IP3 receptor-dependent Ca2+ increases in hippocampal astrocytes does not affect baseline CA1 pyramidal neuron synaptic activity. J Neurosci 28:4967–4973.
51. Okubo Y, Kanemaru K, Suzuki J, Kobayashi K, Hirose K, Iino M (2019): Inositol 1,4,5-trisphosphate receptor type 2-independent Ca^{2+} release from the endoplasmic reticulum in astrocytes. Glia 67:113–124.
52. Shigetomi E, Jackson-Weaver O, Huckstepp RT, O'Dell TJ, Khakh BS (2013): TRPA1 channels are regulators of astrocyte basal calcium levels and long-term potentiation via constitutive D-serine release. J Neurosci 33:10143–10153.
53. Rungta RL, Bernier LP, Dissing-Olesen L, Groten CJ, LeDue JM, Ko R, *et al.* (2016): Ca^{2+} transients in astrocyte fine processes occur via Ca^{2+} influx in the adult mouse hippocampus. Glia 64:2093–2103.
54. Oh SJ, Lee JM, Kim HB, Lee J, Han S, Bae JY, *et al.* (2019): Ultrasonic neuromodulation via astrocytic TRPA1 [published correction appears in Curr Biol 2020; 30:948. Curr Biol 29:3386–3401.e8.
55. Benneyworth MA, Li Y, Basu AC, Bolshakov VY, Coyle JT (2012): Cell selective conditional null mutations of serine racemase demonstrate a predominate localization in cortical glutamatergic neurons. Cell Mol Neurobiol 32:613–624.
56. Sason H, Billard JM, Smith GP, Safory H, Neame S, Kaplan E, *et al.* (2017): Asc-1 transporter regulation of synaptic activity via the tonic release of d-serine in the forebrain. Cereb Cortex 27:1573–1587.
57. Papouin T, Dunphy JM, Tolman M, Dineley KT, Haydon PG (2017): Septal cholinergic neuromodulation tunes the astrocyte-dependent gating of hippocampal NMDA receptors to wakefulness. Neuron 94:840–854.e7.
58. Henneberger C, Papouin T, Oliet SHR, Rusakov DA (2010): Long-term potentiation depends on release of D-serine from astrocytes. Nature 463:232–236.
59. Rosenberg D, Artoul S, Segal AC, Kolodney G, Radzishevsky I, Dikopoltsev E, *et al.* (2013): Neuronal D-serine and glycine release via the Asc-1 transporter regulates NMDA receptor-dependent synaptic activity. J Neurosci 33:3533–3544.
60. Citri A, Malenka RC (2008): Synaptic plasticity: Multiple forms, functions, and mechanisms. Neuropsychopharmacology 33:18–41.
61. Nabavi S, Kessels HW, Alfonso S, Aow J, Fox R, Malinow R (2013): Metabotropic NMDA receptor function is required for NMDA receptor-dependent long-term depression. Proc Natl Acad Sci U S A 110:4027–4032.
62. Ottestad-Hansen S, Hu QX, Follin-Arbelet VV, Bentea E, Sato H, Massie A, *et al.* (2018): The cystine-glutamate exchanger (xCT, Slc7a11) is expressed in significant concentrations in a subpopulation of astrocytes in the mouse brain. Glia 66:951–970.
63. Araque A, Li N, Doyle RT, Haydon PG (2000): SNARE protein-dependent glutamate release from astrocytes. J Neurosci 20:666–673.
64. Han YE, Kwon J, Won J, An H, Jang MW, Woo J, *et al.* (2019): Tweety-homolog (Ttyh) family encodes the pore-forming subunits of the swelling-dependent volume-regulated anion channel (VRACswell) in the brain. Exp Neurobiol 28:183–215.
65. Yang J, Vitery MDC, Chen J, Osei-Owusu J, Chu J, Qiu Z (2019): Glutamate-releasing SWELL1 channel in astrocytes modulates synaptic transmission and promotes brain damage in stroke. Neuron 102:813–827.e6.
66. Lalo U, Rasooli-Nejad S, Bogdanov A, More L, Koh W, Muller J, *et al.* (2021): Synergy between vesicular and non-vesicular gliotransmission regulates synaptic plasticity and working memory. bioRxiv. https://doi.org/10.1101/2021.03.25.437028.
67. Povysheva NV, Johnson JW (2012): Tonic NMDA receptor-mediated current in prefrontal cortical pyramidal cells and fast-spiking interneurons. J Neurophysiol 107:2232–2243.
68. Ghersi C, Bonfanti A, Manzari B, Feligioni M, Raiteri M, Pittaluga A (2003): Pharmacological heterogeneity of release-regulating presynaptic AMPA/kainate receptors in the rat brain: Study with receptor antagonists. Neurochem Int 42:283–292.
69. Atzori M, Cuevas-Olguin R, Esquivel-Rendon E, Garcia-Oscos F, Salgado-Delgado RC, Saderi N, *et al.* (2016): Locus ceruleus norepinephrine release: A central regulator of CNS spatio-temporal activation? Front Synaptic Neurosci 8:25.
70. Jacobowitz DM (1979): Hypothesis for the local control of norepinephrine release. In: Usdin E, Kopin IJ, Barchas J, editors. Catecholamines: Basic and Clinical Frontiers, Proceedings of the Fourth International Catecholamine Symposium, Pacific Grove, California, September 17-22, 1978. New York: Pergamon, 1792–1794.
71. Serrano A, Haddjeri N, Lacaille JC, Robitaille R (2006): GABAergic network activation of glial cells underlies hippocampal heterosynaptic depression. J Neurosci 26:5370–5382.
72. Bushong EA, Martone ME, Jones YZ, Ellisman MH (2002): Protoplasmic astrocytes in CA1 stratum radiatum occupy separate anatomical domains. J Neurosci 22:183–192.
73. Kim JI, Lee HR, Sim SE, Baek J, Yu NK, Choi JH, *et al.* (2011): PI3Kγ is required for NMDA receptor-dependent long-term depression and behavioral flexibility. Nat Neurosci 14:1447–1454.
74. Dong Z, Bai Y, Wu X, Li H, Gong B, Howland JG, *et al.* (2013): Hippocampal long-term depression mediates spatial reversal learning in the Morris water maze. Neuropharmacology 64:65–73.
75. Do-Monte FHM, Allensworth M, Carobrez AP (2010): Impairment of contextual conditioned fear extinction after microinjection of alpha-1-adrenergic blocker prazosin into the medial prefrontal cortex. Behav Brain Res 211:89–95.
76. Homan P, Lin Q, Murrough JW, Soleimani L, Bach DR, Clem RL, Schiller D (2017): Prazosin during threat discrimination boosts memory of the safe stimulus. Learn Mem 24:597–601.
77. Boone KB, Ghaffarian S, Lesser IM, Hill-Gutierrez E, Berman NG (1993): Wisconsin Card Sorting Test performance in healthy, older adults: Relationship to age, sex, education, and IQ. J Clin Psychol 49:54–60.
78. Dezfuli G, Martin L, Olson T, Kellar KJ (2019): The decline of glutamate-stimulated norepinephrine release in aging rat brain. FASEB J 33.. 501.511–501.511.
79. Matchett BJ, Grinberg LT, Theofilas P, Murray ME (2021): The mechanistic link between selective vulnerability of the locus coeruleus and neurodegeneration in Alzheimer's disease. Acta Neuropathol 141:631–650.